

A Poisson Model for Entanglement Optimization in the Quantum Internet

Laszlo Gyongyosi

Abstract—A Poisson model for entanglement optimization in quantum repeater networks is defined in this paper. The nature-inspired multiobjective optimization framework fuses the fundamental concepts of quantum Shannon theory with the theory of evolutionary algorithms. The optimization model aims to maximize the entanglement fidelity and relative entropy of entanglement for all entangled connections of the quantum network. The cost functions are subject of a minimization defined to cover and integrate the physical attributes of entanglement transmission, purification, and storage of entanglement in quantum memories. The method can be implemented with low complexity that allows a straightforward application in future quantum Internet and quantum networking scenarios.

Index Terms—quantum networking; quantum repeater; quantum entanglement; quantum Internet; quantum Shannon theory.

I. INTRODUCTION

Quantum entanglement serves as a fundamental concept of long-distance quantum networks, quantum Internet, and future quantum communications [1]–[4], [7]. Since the no-cloning theorem makes it impossible to use the “copy-and-resend” mechanisms of traditional repeaters [7], in a quantum networking scenario the quantum repeaters have to transmit correlations in a different way [1]–[5]. The main task of quantum repeaters is to distribute quantum entanglement between distant points that will then serve as a fundamental base resource for quantum teleportation and other quantum protocols [1]. Since in an experimental scenario [15]–[21] the quantum links between nodes are noisy and entanglement fidelity decreases as hop distance increases, entanglement purification is applied to improve the entanglement fidelity between nodes [1], [3]–[6]. Quantum nodes also perform internal quantum error correction that is a requirement for reliability and storage in quantum memories [1], [5], [6], [8]. Both entanglement purification and quantum error correction steps in local nodes are high-cost tasks that require significant minimization [1], [3]–[6], [15], [16], [19]–[21].

The shared entangled connections between nodes form entangled links. Significant attributes of these entangled links

are entanglement fidelity, and correlation, in terms of relative entropy entanglement (for a definition, see Section A). Entanglement fidelity is a crucial parameter. It serves as the primary objective function in our model, which is a subject of maximization. Maximizing the relative entropy of entanglement is the secondary objective function. Minimizing the cost of classical communications, which is required by the entanglement optimization method as an auxiliary objective function, is also considered.

Besides these attributes, the entangled links are characterized by the entanglement throughput that identifies the number of transmittable entangled systems per sec at a particular fidelity. In our model, the nodes are associated with an incoming entanglement throughput [1], that serves as a resource for the nodes to maximize the entanglement fidelity and the relative entropy of entanglement. The nodes receive and process the incoming entangled states. Each node performs purification and internal quantum error correction, and it stores the entangled systems in local quantum memories. The amount of input entangled systems in a node is therefore connected to the achievable maximal entanglement fidelity and correlation in the entangled states associated with that node. The objective of the proposed model is to reveal this connection and to define a framework for entanglement optimization in the quantum nodes of an arbitrary quantum network. The required input information for the optimization without loss of generality are the number of nodes, the number of fidelity types of the received entangled states, and the node characteristics. In a realistic setting, these cover the incoming entanglement throughput in a node and the costs of internal entanglement purification steps, internal quantum error corrections, and quantum memory usage.

In this work, an optimization framework for quantum networks is defined. The method aims to maximize the achievable entanglement fidelity and correlation of entangled systems, in parallel with the minimization of the cost of entanglement purification and quantum error correction steps in the quantum nodes of the network. The problem model is therefore defined as a multiobjective optimization. This paper aims to provide a model that utilizes the realistic parameters of the internal mechanisms of the nodes and the physical attributes of entanglement transmission. The proposed framework integrates the results of quantum Shannon theory, the theory of evolutionary multiobjective optimization algorithms [9], [10], and the mathematical modeling of seismic wave propagation [9]–[14].

Inspired by the statistical distribution of seismic events and the modeling of wave propagations in nature, the model uti-

This work was partially supported by the European Research Council through the Advanced Fellow Grant, in part by the Royal Society’s Wolfson Research Merit Award, in part by the Engineering and Physical Sciences Research Council under Grant EP/L018659/1, by the Hungarian Scientific Research Fund - OTKA K-112125, and by the National Research Development and Innovation Office of Hungary (Project No. 2017-1.2.1-NKP-2017-00001).

L. Gyongyosi is with the School of Electronics and Computer Science, University of Southampton, Southampton SO17 1BJ, U.K., also with the Department of Networked Systems and Services, Budapest University of Technology and Economics, 1117 Budapest, Hungary, and also with the MTA-BME Information Systems Research Group, Hungarian Academy of Sciences, 1051 Budapest, Hungary (e-mail: l.gyongyosi@soton.ac.uk)

lizes a Poisson distribution framework to find optimal solutions in the objective space. In the theory of earthquake analysis and spatial connection theory [9]–[14], Poisson distributions are crucial in finding new epicenters. Motivated by these findings, a Poisson model is proposed to find new solutions in the objective space that is defined by the multiobjective optimization problem. The solutions in the objective space are represented by epicenters with several locations around them that also represent solutions in the feasible space [9], [10]. The epicenters have a magnitude and seismic power operators that determine the distributions of the locations and fitness [9], [10] of locations around the epicenters. Epicenters with low magnitude generate high seismic power in the locations, whereas epicenters with high magnitude generate low seismic power in the locations. Epicenters are generated randomly in the feasible space, and each epicenter is weighted from which the magnitude and power are derived. By a general assumption, epicenters with lower magnitude produce more locations because the locations are closer to the epicenter. The locations are placed within a certain magnitude around the epicenters in the feasible space. The optimization framework involves a set of solutions to the Pareto optimal front by combining the concept of Pareto dominance and seismic wave propagations. The new epicenters are determined by a Poisson distribution in analogue to prediction theory in earthquake models. The mathematical model of epicenters allows us to find new solutions iteratively and to find a global optimum. The framework has low complexity that allows an efficient practical implementation to solve the defined multiobjective optimization problem.

The multiobjective optimization problem model considers the fidelity and correlation of entanglement of entangled states available in the quantum nodes. The resources for the nodes are the incoming entangled states from the quantum links, and the already stored entangled quantum systems in the local quantum memories. In the optimization procedure, both memory consumptions and environmental effects, such as entanglement purification and quantum error correction steps, are considered to develop the cost functions. In particular, the amount of resource, in terms of number of available entangled systems, is a coefficient that can be improved by increasing the incoming number of entangled systems, such as the incoming entanglement throughput in a node. In the proposed model, the incoming entanglement fidelity is further divided into some classes, which allows us to differentiate the resources in the nodes with respect to their fidelity types. Therefore, the fidelity type serves as a quality index for the optimization procedure. The optimization aims to find the optimal incoming entanglement throughput for all nodes that leads to a maximization of entanglement fidelity and correlation of entangled states with respect to the relative entropy of entanglement, for all entangled connections in the quantum network.

The novel contributions of this paper are as follows:

- A nature-inspired, multiobjective optimization framework is conceived for quantum repeater networks.
- The model considers the physical attributes of entanglement transmission and quantum memories to provide

a realistic setting (realistic objective functions and cost functions).

- The method fuses the results of quantum Shannon theory and theory of evolutionary multiobjective optimization algorithms.
- The model maximizes the entanglement fidelity and relative entropy of entanglement for all entangled connections of the network. It minimizes the cost functions to reduce the costs of entanglement purification, error correction, and quantum memory usage.
- The optimization framework allows a low-complexity implementation.

This paper is organized as follows. Section II presents the problem statement. Section III details the optimization method. Section IV provides the problem resolution. Section V proposes numerical evidence. Finally, Section VI concludes the paper. Supplemental material is included in the Appendix.

II. PROBLEM STATEMENT

The problem statement is as follows. For a given quantum network with N nodes, for all nodes x_i , $i = 1, \dots, N$, the entanglement fidelity and relative entropy of entanglement for all entangled connections are maximized, and the cost of optimal purification and quantum error correction and the cost of memory usage for all nodes are minimized.

The network model is as follows: Let $B_F(x)$ be the incoming number of received entangled states (incoming entanglement throughput) in a given quantum node x , measured in the number of d -dimensional entangled states per sec at a particular entanglement fidelity F [1], [3], [4].

Let N be the number of nodes in the network, and let T be the number of fidelity types F_j , $j = 1, \dots, T$ of the entangled states in the quantum network.

Let $B_F^j(x_i)$ be the number of incoming entangled states in an i^{th} node x_i , $i = 1, \dots, N$, from fidelity type j . In our model, $B_F^j(x_i)$ represents the utilizable resources in a particular node x_i . Thus, the task is to determine this value for all nodes in the quantum network to maximize the fidelity and relative entropy of shared entanglement for all entangled connections.

Let \mathbf{X} be an $N \times T$ matrix

$$\mathbf{X} = \left(B_F^j(x_i) \right)_{N \times T}. \quad (1)$$

The matrix describes the number of entangled states of each fidelity type for all nodes in the network, $B_F^j(x_i) \geq 0$ for all i and j .

A. Objective Functions

For a given node x_i , let $\mathcal{F}(x_i)$ be the primary objective function that identifies the cumulative entanglement fidelity (a sum of entanglement fidelities in x_i) after an entanglement purification $P(x_i)$ and an optimal quantum error correction $C(x_i)$ in x_i . In our framework, $\mathcal{F}_i(\mathbf{X})$ for a node x_i is defined as

$$\mathcal{F}_i(\mathbf{X}) = \sum_{j=1}^T \sum_{k=1}^T A_{ijk} \tilde{B}_F^j(x_i) \tilde{B}_F^k(x_i) + \sum_{j=1}^T R_{ij} \tilde{B}_F^j(x_i) + c_i, \quad (2)$$

where A_{ijk} is the quadratic regression coefficient, R_{ij} is the simple regression coefficient, c_i is a constant, and $\tilde{B}_F^j(x_i)$ is defined as

$$\tilde{B}_F^j(x_i) = B_F^j(x_i) + \langle B \rangle_F^j(x_i), \quad (3)$$

where $\langle B \rangle_F^j(x_i)$ is an initialization value for $B_F^j(x_i)$ in a particular node x_i .

Then let $\mathbb{E}(D_i(\mathbf{X}))$ be the secondary objective function that refers to the expected amount of cumulative relative entropy of entanglement (a sum of relative entropy of entanglement) in node x_i , defined as

$$\begin{aligned} \mathbb{E}(D_i(\mathbf{X})) &= \sum_{j=1}^T \sum_{k=1}^T A_{ijk}^* \tilde{B}_F^j(x_i) \tilde{B}_F^k(x_i) \\ &\quad + \sum_{j=1}^T R_{ij}^* \tilde{B}_F^j(x_i) + c_i^*, \end{aligned} \quad (4)$$

where A_{ijk}^* , R_{ij}^* , and c_i^* are some regression coefficients, by definition.

Therefore, the aim is to find the values of $B_F^j(x_i)$ for all i and j in (1), such that $\mathcal{F}_i(\mathbf{X})$ and $\mathbb{E}(D_i(\mathbf{X}))$ are maximized for all i .

Assuming that the fidelity of entanglement is dynamically changing and evolves over time, the $w_j(x_i)$ quantum memory coefficient is introduced for the storage of entangled states from the j^{th} fidelity type in a node x_i as follows:

$$w_j(x_i) = \eta_j B_F^j(x_i) + \kappa_j \langle B \rangle_F^j(x_i), \quad (5)$$

where η_j and κ_j are coefficients that describe the storage characteristic of entangled states with the j^{th} fidelity type.

B. Cost Functions

The cumulative entanglement fidelity (2) and cumulative relative entropy of entanglement (4) in a particular node x_i are associated with a $f_C(P(x_i))$ cost entanglement purification $P(x_i)$ and a $f_C(C(x_i))$ cost of optimal quantum error correction $C(x_i)$ in x_i , where $f_C(\cdot)$ is the cost function.

Then let $\mathcal{C}(\mathbf{X})$ be the total cost function for all of the T fidelity types and for all of the N nodes, as follows:

$$\begin{aligned} \mathcal{C}(\mathbf{X}) &= \sum_{i=1}^N f_C(P(x_i)) + f_C(C(x_i)) \\ &= \sum_{i=1}^N \sum_{j=1}^T f_j B_F^j(x_i), \end{aligned} \quad (6)$$

where f_j is a total cost of purification and error correction associated with the j^{th} fidelity type of entangled states.

Let F^* be a critical fidelity on the received quantum states. The entangled states are then decomposable into two sets \mathcal{S}_{low} and \mathcal{S}_{high} with fidelity bounds $\mathcal{S}_{low}(F)$ and $\mathcal{S}_{high}(F)$ as

$$\mathcal{S}_{low}(F) : \max_{\forall i} F_i < F^*, \quad (7)$$

and

$$\mathcal{S}_{high}(F) : \min_{\forall i} F_i \geq F^*. \quad (8)$$

For the quantum systems of \mathcal{S}_{low} , the highest fidelity is below the critical amount F^* , and for set \mathcal{S}_{high} , the lowest fidelity

is at least F^* . Then let $X_{\mathcal{S}_{low}}$ and $X_{\mathcal{S}_{high}}$ identify the set of nodes for which condition (7) or (8) holds, respectively.

Let $\mathcal{S}_i(\mathbf{X})$ be the cost of quantum memory usage in node x_i , defined as

$$\mathcal{S}_i(\mathbf{X}) = \lambda \sum_{j=1}^T \alpha_i \frac{1}{\Upsilon_i} B_F^j(x_i), \quad (9)$$

where λ is a constant, α_i is a quality coefficient that identifies set (7) or (8) for a given node x_i , and Υ_i is the capacity coefficient of the quantum memory.

The main components of the network model are depicted in Fig. 1.

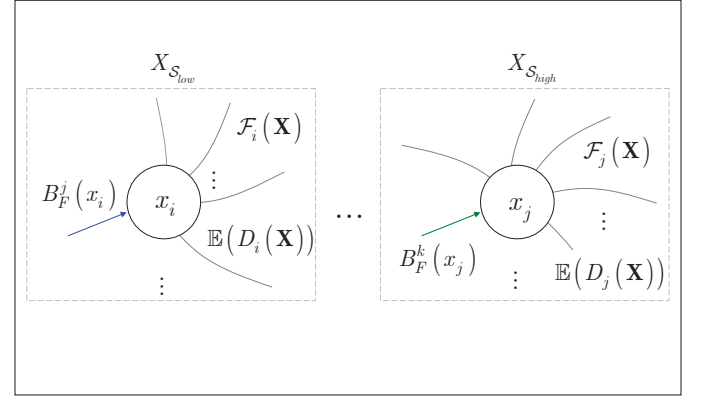


Fig. 1. Illustration of the network model components. The quantum nodes x_i and x_j are associated with current input values $B_F^j(x_i)$ and $B_F^l(x_j)$ (blue and green arrows), where j and l identify the fidelity types of received entangled states. The nodes have several entangled connections (depicted by gray lines) in the network. The nodes are associated with subject functions $\mathcal{F}_i(\mathbf{X})$, $\mathbb{E}(D_i(\mathbf{X}))$, and $\mathcal{F}_j(\mathbf{X})$, $\mathbb{E}(D_j(\mathbf{X}))$. The maximum of the received entanglement fidelity in the nodes allows the classification of the nodes to sets $X_{\mathcal{S}_{low}}$ and $X_{\mathcal{S}_{high}}$: node x_i belongs to set $X_{\mathcal{S}_{low}}$, whereas node x_j belongs to set $X_{\mathcal{S}_{high}}$ (depicted by dashed frames).

C. Multiobjective Optimization

The optimization problem is as follows: the entanglement fidelity and the relative entropy of entanglement for all types of fidelity of stored entanglement for all nodes are maximized, while the cost of entanglement purification and quantum error correction is minimal, and the memory usage cost (required storage time) is also minimal. These requirements define a multiobjective optimization problem [9], [10].

Utilizing functions (2) and (4), the function subject of a maximization to yield maximal entanglement fidelity and maximal relative entropy of entanglement in all nodes of the network is defined via main objective function $\mathcal{G}(\mathbf{X})$:

$$\mathcal{G}(\mathbf{X}) = \max \sum_{i=1}^N \mathcal{F}_i(\mathbf{X}) \mathbb{E}(D_i(\mathbf{X})). \quad (10)$$

Function $\mathcal{G}(\mathbf{X})$ should be maximized while cost functions (6) and (9) are minimized via functions $F_1(N)$ and $F_2(N)$:

$$F_1(N) = \min \mathcal{C}(\mathbf{X}) = \sum_{i=1}^N \sum_{j=1}^T f_j B_F^j(x_i), \quad (11)$$

and

$$F_2(N) = \min \mathcal{S}(\mathbf{X}) = \sum_{i=1}^N \mathcal{S}_i(\mathbf{X}), \quad (12)$$

with the problem constraints [9], [10] C_1 , C_2 , and C_3 for all i and j . Constraint C_1 is defined as

$$C_1 : \zeta(\mathbf{X}) \geq \gamma, \quad (13)$$

where γ is a cumulative lower bound on the required entanglement fidelity for all nodes, while $\zeta(\mathbf{X})$ is

$$\zeta(\mathbf{X}) = \sum_{i=1}^N \mathcal{F}_i(\mathbf{X}), \quad (14)$$

and constraint C_2 is

$$C_2 : \mathbf{X} \leq \Lambda, \quad (15)$$

where Λ is an upper bound on the total cost function $\mathcal{C}(\mathbf{X})$, while \mathbf{X} is

$$\mathbf{X} = \sum_{i=1}^N \sum_{j=1}^T f_j B_F^j(x_i). \quad (16)$$

For constraint C_3 , let $\tau_j(\mathbf{X})$ be a differentiation of storage characteristic of entangled states from the j^{th} fidelity type:

$$\tau_j(\mathbf{X}) = \sum_{i=1}^N (w_j(x_i) - \Omega)^2, \quad (17)$$

where

$$\Omega = \frac{\sum_{i=1}^N w_j(x_i)}{N}. \quad (18)$$

Then, C_3 is defined as

$$C_3 : \nu(\mathbf{X}) \leq \Pi, \quad (19)$$

where Π is an upper bound on the storage characteristic of entangled states from the j^{th} fidelity type, while ν is evaluated via (17) as

$$\nu = \sum_{j=1}^T \tau_j(\mathbf{X}). \quad (20)$$

III. POISSON MODEL FOR ENTANGLEMENT OPTIMIZATION

This section defines the Poisson entanglement optimization method, and it is applied to the solution of the multiobjective optimization problem of Section II.

A. Poisson Operators

The attributes of the Poisson operator are as follows:

1) *Dispersion*: The $D(\mathcal{E})$ dispersion coefficient of an epicenter \mathcal{E} (solution in the feasible space \mathcal{S}_F) determines the number of affected L_j , $j = 1, \dots, D(\mathcal{E})$, locations around an epicenter \mathcal{E} . The random locations around an epicenter also represent solutions in \mathcal{S}_F that help in increasing the diversity of population \mathcal{P} (a set of possible solutions) to find a global optimum. The diversity increment is therefore a tool to avoid an early convergence to a local optimum [9], [10].

The dispersion $D(\mathcal{E}_i)$ operator for an i^{th} epicenter \mathcal{E}_i is defined as

$$D(\mathcal{E}_i) = m \frac{(\tilde{f}(\langle \mathcal{E} \rangle) - \tilde{f}(\mathcal{E}_i)) + \vartheta}{\sum_{i=1}^{|\mathcal{P}|} (\tilde{f}(\langle \mathcal{E} \rangle) - \tilde{f}(\mathcal{E}_i)) + \vartheta}, \quad (21)$$

where m is a control parameter, \mathcal{E}_i is an i^{th} individual (epicenter) from the $|\mathcal{P}|$ individuals (epicenters) in population \mathcal{P} , $|\mathcal{P}|$ is the size of population \mathcal{P} , function $\tilde{f}(\cdot)$ is the fitness value (see Section B1), $\tilde{f}(\langle \mathcal{E} \rangle)$ is a maximum objective value among the $|\mathcal{P}|$ individuals, and ϑ is a residual quantity.

Without loss of generality, assuming $|\mathcal{P}|$ epicenters, the q total number of locations is as

$$q = \sum_{i=1}^{|\mathcal{P}|} D(\mathcal{E}_i). \quad (22)$$

2) *Seismic Power and Magnitude*: Assume that L_j is a random location around \mathcal{E}_i . For L_j , the Euclidean distance $d(\mathcal{E}_i, l_j)$ between an i^{th} epicenter \mathcal{E}_i and the projection point l_j of a j^{th} location point L_j , $j = 1, \dots, D(\mathcal{E})$ on the ellipsoid around \mathcal{E}_i is as follows:

$$\begin{aligned} d(\mathcal{E}_i, l_j) &= \sqrt{(\dim_1(l_j))^2 + (\dim_2(l_j))^2} \\ &= \sqrt{\frac{1 + tg^2 \alpha_{\mathcal{E}_i}(l_j)}{a^{-2} + tg^2 \alpha_{\mathcal{E}_i}(l_j)}}, \end{aligned} \quad (23)$$

where $\dim_i(\cdot)$ is the i^{th} dimension of l_j , and

$$\frac{(\dim_1(l_j))^2}{a^2} + \frac{(\dim_2(l_j))^2}{b^2} = 1, \quad (24)$$

where coefficients a and b define the shape of the ellipse around epicenter \mathcal{E}_i (see Fig. 2), while $\alpha_{\mathcal{E}_i}(l_j)$ is an angle:

$$tg \alpha_{\mathcal{E}_i}(l_j) = \frac{\dim_2(l_j)}{\dim_1(l_j)}. \quad (25)$$

The seismic power $P(\mathcal{E}_i, L_j)$ operator for an i^{th} epicenter \mathcal{E}_i in a j^{th} location point L_j , $j = 1, \dots, D(\mathcal{E}_i)$ is defined as

$$P(\mathcal{E}_i, L_j) = \left(\frac{1}{d(\mathcal{E}_i, l_j)} M(\mathcal{E}_i, L_j) \right)^{b_1} b_0 e^{\sigma_{\ln P(\mathcal{E}_i, L_j)}}, \quad (26)$$

where b_0 and b_1 are regression coefficients, $\sigma_{\ln P(\mathcal{E}_i)}$ is the standard deviation [14], $M(\mathcal{E}_i, L_j)$ is the seismic magnitude in a location L_j , and l_j is the projection of L_j onto the ellipsoid around \mathcal{E}_i [14].

Thus, at a given L_j with $d(\mathcal{E}_i, l_j)$ ((23)), from $P(\mathcal{E}_i, L_j)$ (see (26)), the magnitude $M(\mathcal{E}_i, L_j)$ between epicenter \mathcal{E}_i and location L_j is evaluated as

$$M(\mathcal{E}_i, L_j) = \left(P(\mathcal{E}_i, L_j) \frac{1}{b_0 e^{\sigma_{\ln P(\mathcal{E}_i, L_j)}}} \right)^{\frac{1}{b_1}} d(\mathcal{E}_i, l_j). \quad (27)$$

3) *Cumulative Magnitude*: Let $L_j^{\mathcal{E}_i}$ be the location point where the seismic power $P(\mathcal{E}_i, L_j^{\mathcal{E}_i})$ is maximal for a given epicenter \mathcal{E}_i . Let $P^*(\mathcal{E}_i)$ be the maximal seismic power,

$$P^*(\mathcal{E}_i) = \max_{\forall j} P(\mathcal{E}_i, L_j^{\mathcal{E}_i}). \quad (28)$$

Assuming that $|\mathcal{P}|$ epicenters, $\mathcal{E}_1, \dots, \mathcal{E}_{|\mathcal{P}|}$ exist in the system, let identify by $P_{\max}(\mathcal{E}')$ the epicenter \mathcal{E}' with a maximal seismic power among as

$$P_{\max}(\mathcal{E}') = \max_{\forall i} (P^*(\mathcal{E}_i)), \quad (29)$$

with magnitude $M(\mathcal{E}', L_j^{\mathcal{E}'})$, where $L_j^{\mathcal{E}'}$ is the location point where the seismic power $P_{\max}(\mathcal{E}')$ is maximal yielded for \mathcal{E}' .

Then the $C(\mathcal{E}_i)$ cumulative magnitude for an epicenter \mathcal{E}_i is defined as

$$C(\mathcal{E}_i) = \mathcal{M} \frac{(\tilde{f}(\mathcal{E}_i) - \tilde{f}(\mathcal{E}')) + \vartheta}{\sum_{i=1}^{|\mathcal{P}|} (\tilde{f}(\mathcal{E}_i) - \tilde{f}(\mathcal{E}')) + \vartheta}, \quad (30)$$

where \mathcal{E}' is the highest seismic power epicenter with magnitude $M(\mathcal{E}', L_j^{\mathcal{E}'})$, $\tilde{f}(\mathcal{E}')$ is the minimum objective value among the $|\mathcal{P}|$ epicenters, and \mathcal{M} is a control parameter defined as

$$\mathcal{M} = \sum_{i=1}^{|\mathcal{P}|} M(\mathcal{E}_i, L_j^{\mathcal{E}_i}), \quad (31)$$

where $L_j^{\mathcal{E}_i}$ provides the maximal seismic power for an i^{th} epicenter \mathcal{E}_i , functions $\tilde{f}(\mathcal{E}_i)$ and $\tilde{f}(\mathcal{E}')$ are the fitness values (see Section B1) for the current epicenter \mathcal{E}_i and for the highest seismic power epicenter \mathcal{E}' , and ϑ is a residual quantity.

B. Distribution of Epicenters

Assume that \mathcal{E}_i is a current epicenter (solution) and \mathcal{R}_k and \mathcal{R}_l are two random reference points around \mathcal{E}_i . Using the $C(\mathcal{E}_i)$ cumulative seismic magnitude ((30)) of an epicenter \mathcal{E}_i , the generation of a new epicenter \mathcal{E}_p is as follows:

Let $\Phi(\mathcal{E}_i, \mathcal{R}_k, \mathcal{R}_l)$ be a Poisson range identifier function [12], [13] for \mathcal{E}_i using \mathcal{R}_k and \mathcal{R}_l as random reference points:

$$\begin{aligned} \Phi(\mathcal{E}_i, \mathcal{R}_k, \mathcal{R}_l) \\ = \frac{d(\mathcal{E}_i, \mathcal{R}_k) c_w(\mathcal{R}_k, \mathcal{R}_l)}{\cos(\theta(\ell_{\mathcal{E}_i, \mathcal{R}_k}, \ell_{\mathcal{R}_k, \mathcal{R}_l})) \cdot d(\mathcal{R}_k, \mathcal{R}_l) c_w(\mathcal{E}_i, \mathcal{R}_k)}, \end{aligned} \quad (32)$$

where \mathcal{E}_i is a current epicenter, \mathcal{R}_k and \mathcal{R}_l are random reference points, $d(\cdot)$ is the Euclidean distance function, $c_w(\mathcal{E}_i, \mathcal{R}_k)$ and $c_w(\mathcal{R}_k, \mathcal{R}_l)$ are weighting coefficients between epicenters \mathcal{E}_i and \mathcal{R}_k and between \mathcal{R}_k and \mathcal{R}_l , and $\theta(\ell_{\mathcal{E}_i, \mathcal{R}_k}, \ell_{\mathcal{R}_k, \mathcal{R}_l})$ is the angle between lines $\ell_{\mathcal{E}_i, \mathcal{R}_k}$ and $\ell_{\mathcal{R}_k, \mathcal{R}_l}$:

$$\begin{aligned} \theta(\ell_{\mathcal{E}_i, \mathcal{R}_k}, \ell_{\mathcal{R}_k, \mathcal{R}_l}) \\ = \cos^{-1} \left(\frac{d(\mathcal{E}_i, \mathcal{R}_k)^2 + d(\mathcal{E}_k, \mathcal{R}_l)^2 - d(\mathcal{E}_i, \mathcal{R}_l)^2}{2d(\mathcal{E}_i, \mathcal{R}_k) d(\mathcal{R}_k, \mathcal{R}_l)} \right). \end{aligned} \quad (33)$$

Without loss of generality, using (32), a Poissonian distance function $\mathcal{D}(\mathcal{E}_p)$ for the finding of new epicenter \mathcal{E}_p is defined via a P Poisson distribution [12], [13] as follows:

$$\mathcal{D}(\mathcal{E}_p) = P(k, \lambda), \quad (34)$$

where

$$k = \Phi(\mathcal{E}_i, \mathcal{R}_k, \mathcal{R}_l), \quad (35)$$

with mean

$$\lambda = \mathbb{E}[\Phi(\mathcal{E}_i, \mathcal{R}_k, \mathcal{R}_l)]. \quad (36)$$

Therefore, the resulting new epicenter \mathcal{E}_p is a Poisson random epicenter \mathcal{E}_p with a Poisson range identifier $\mathcal{D}(\mathcal{E}_p)$.

For a large set of reference points, only those reference points that are within the $r(\mathcal{E}_i)$ radius around the current solution \mathcal{E}_i are selected for the determination of the new solution \mathcal{E}_p . This radius is defined as

$$r(\mathcal{E}_i) = \chi 10^{Q_1(2\tilde{M}) - Q_2}, \quad (37)$$

where \tilde{M} is the average magnitude,

$$\tilde{M} = \frac{1}{|\mathcal{P}|} \mathcal{M} = \frac{1}{|\mathcal{P}|} \sum_{i=1}^{|\mathcal{P}|} M(\mathcal{E}_i, L_j^{\mathcal{E}_i}), \quad (38)$$

Q_1 and Q_2 are constants, and χ is a normalization term. Motivated by the corresponding seismologic relations of the Dobrovolsky-Megathrust radius formula [13], the constants in (37) are selected as $Q_1 = 0.414$ and $Q_2 = 1.696$.

In the relevance range $r(\mathcal{E}_i)$ of (37), the weights of reference points are determined by the seismic power function (26).

C. Population Diversity

1) *Hypocentral*: The hypocentral of an epicenter is aimed to increase the diversity of population by a randomization.

Let $\dim_k(\mathcal{E}_i)$ be an actual randomly selected k^{th} dimension and $k = 1, \dots, \dim(\mathcal{E}_i)$ be a current epicenter \mathcal{E}_i , $i = 1, \dots, |\mathcal{P}|$. The $\mathcal{H}(\dim_k(\mathcal{E}_i))$ hypocentral provides a random displacement [12], [13] of $\dim_k(\mathcal{E}_i)$ using $C(\mathcal{E}_i)$ (see (30)):

$$\begin{aligned} \mathcal{H}(\dim_k(\mathcal{E}_i)) = \dim_k(\mathcal{E}_i') \\ = \sqrt{\left(\frac{1}{M(\dim_k(\mathcal{E}_i), L_j^{\dim_k(\mathcal{E}_i)})} \dim_k(\mathcal{E}_i) \right)^2 + (\mathcal{U}(-C(\mathcal{E}_i), C(\mathcal{E}_i)))^2} \end{aligned} \quad (39)$$

where $\mathcal{U}(-C(\mathcal{E}_i), C(\mathcal{E}_i))$ is a uniform random number from the range of $[-C(\mathcal{E}_i), C(\mathcal{E}_i)]$ to yield the displacement $\dim_k(\mathcal{E}_i')$, $M(\dim_k(\mathcal{E}_i), L_j^{\dim_k(\mathcal{E}_i)})$ is the magnitude, and $L_j^{\dim_k(\mathcal{E}_i)}$ is a location point where $P(\dim_k(\mathcal{E}_i), L_j^{\dim_k(\mathcal{E}_i)})$ is maximal for $\dim_k(\mathcal{E}_i)$.

The $D(\mathcal{E}_i)$ locations around the cumulative magnitude $C(\mathcal{E}_i)$ of \mathcal{E}_i are generated by (39) through all the randomly selected Y dimensions, where Y is as follows [9], [10]:

$$Y = \mathcal{U}(1, \dim(\mathcal{E}_i)). \quad (40)$$

The process is repeated for all \mathcal{E}_i .

2) *Poisson Randomization*: To generate random locations around $\text{dim}_k(\mathcal{E}_i)$, a Poisson distribution is also used to increase the diversity of the population. A random location in the k^{th} dimension $L_r^{\text{dim}_k(\mathcal{E}_i)}$ around $\text{dim}_k(\mathcal{E}_i)$ is generated as follows:

$$L_r^{\text{dim}_k(\mathcal{E}_i)} = \text{dim}_k(\mathcal{E}_i) w, \quad (41)$$

where

$$w \in P(X = k, \lambda) \quad (42)$$

is a Poisson random number with distribution coefficients k and λ . Given that it is possible that using (41) some randomly generated locations will be out of the feasible space S_F , a normalization operator $N(\cdot)$ of $L_r^{\text{dim}_k(\mathcal{E}_i)}$ is defined to keep the new locations around $\text{dim}_k(\mathcal{E}_i)$ in S_F , as follows [9], [10]:

$$L_r^{\text{dim}_k(\mathcal{E}_i)} = L_r^{\text{dim}_k(\mathcal{E}_i)} (\text{mod}(B_{up}^k - B_{low}^k)) + B_{low}^k, \quad (43)$$

where B_{low}^k and B_{up}^k are lower and upper bounds on the boundaries of locations in a k^{th} dimension, and $\text{mod}(\cdot)$ is to a modular arithmetic function. The procedure is repeated for the randomly selected $t = \mathcal{U}(1, \text{dim}(\mathcal{E}_i))$ dimensions of \mathcal{E}_i , for $\forall i$.

D. Iterative Convergence

The method of convergence of solutions in the Poisson optimization is summarized in Method 1.

Method 1 Convergence of Solutions

- Step 1.** Generate $|\mathcal{P}|$ epicenters, $\mathcal{E}_1, \dots, \mathcal{E}_{|\mathcal{P}|}$, with $D(\mathcal{E}_i)$ random locations around a given i^{th} epicenter \mathcal{E}_i .
 - Step 2.** Select an epicenter \mathcal{E}_i , and determine the seismic operators $D(\mathcal{E}_i)$, $P(\mathcal{E}_i, L_j)$, $M(\mathcal{E}_i, L_j)$.
 - Step 3.** Determine the $\mathfrak{D}(\mathcal{E}_p)$ Poisson distance function using references \mathcal{R}_k and \mathcal{R}_l to yield a new solution \mathcal{E}_p .
 - Step 4.** Repeat steps 1–3, until the closest epicenter to the \mathcal{E}' optimal epicenter is not found or other stopping criteria are not met.
-

An epicenter \mathcal{E}_i and the generation of a new solution \mathcal{E}_p with an in the objective space S_O are depicted in Fig. 2. The ellipsoid around \mathcal{E}_i and the projection point l_k of the reference location \mathcal{R}_k are serving the determination of power function $P(\mathcal{E}_i, \mathcal{R}_k)$ in the reference location \mathcal{R}_k .

A new epicenter \mathcal{E}_p is determined via the Poisson function $\mathfrak{D}(\mathcal{E}_p)$. Locations with low power function (26) values have high magnitudes (27) from the epicenter, whereas locations with high power function values have low magnitudes from the epicenter.

E. Framework

The algorithmical framework that utilizes the Poisson entanglement optimization method for the problem statement presented in Section II is defined in Algorithm 1.

Sub-procedure 1 of step 5 is discussed in the Appendix.

Algorithm 1 Poisson Entanglement Optimization for Quantum Networks

- Step 0.** In an initial phase, a random population \mathcal{P} of $|\mathcal{P}|$ feasible solutions is generated [9], [10] Let G be an upper bound on the number of generations, n_G .
 - Step 1.** For each epicenter $x_i = \mathcal{E}_i$ in \mathcal{P} , define $D(\mathcal{E}_i)$ random locations around \mathcal{E}_i . For a diversity increment, determine the $\mathcal{H}(\text{dim}_k(\mathcal{E}_i))$ hypocentral displacement function (39) for $\text{dim}_k(\mathcal{E}_i)$, for $k = 1, \dots, \text{dim}(\mathcal{E}_i)$.
 - Step 2.** Determine the seismic power $P(\mathcal{E}_i, L_j)$ operator via (26) for an i^{th} epicenter \mathcal{E}_i in a j^{th} location point $L_j, j = 1, \dots, D(\mathcal{E}_i)$. Determine the $L_j^{\mathcal{E}_i}$, the location point where the seismic power $P(\mathcal{E}_i, L_j^{\mathcal{E}_i})$ is maximal for a given epicenter \mathcal{E}_i , via (28).
 - Step 3.** Determine epicenter \mathcal{E}' with a maximal seismic power $P_{\max}(\mathcal{E}')$ via (29). Compute seismic magnitude $M(\mathcal{E}', L_j^{\mathcal{E}'})$ via (27), and determine the sum of all N seismic magnitudes \mathcal{M} via (31).
 - Step 4.** Compute the $D(\mathcal{E}_i)$ dispersion via (21) and the $C(\mathcal{E}_i)$ cumulative seismic magnitude via (30). Select non-dominated solutions from the \mathcal{P} population set to the set \mathcal{NP} of non-dominated solutions. Identify φ_k as $\varphi_k = L_k^{\mathcal{E}_i}$, where $L_k^{\mathcal{E}_i}$ is a k^{th} location around \mathcal{E}_i . Update \mathcal{NP} with the non-dominated solutions.
 - Step 5.** Create set \mathcal{P}' of epicenters by selecting p feasible solutions from \mathcal{P} using the $\text{Pr}(\varphi_i)$ selection probability as $\text{Pr}(\varphi_i) = \tilde{f}(\varphi_i) / \sum_{r \in \mathcal{P}} \tilde{f}(\varphi_r)$. Apply Sub-procedure 1.
 - Step 6.** If $n_G \geq G$, then stop the iteration; otherwise, repeat steps 1–4.
-

1) *Optimization of Classical Communications*: To achieve the minimization of classical communications required by the entanglement optimization, the S -metric (or hypervolume indicator) is integrated, which is a quality measure for the solutions or a contribution of a single solution in a solution set [9], [10] By definition, this metric identifies the size of dominated space (size of space covered).

By theory, the $S(\mathcal{R})$ S -metric for a solution set $\mathcal{R} = \{r_1, \dots, r_n\}$ is as follows:

$$S(\mathcal{R}) = \mathcal{L} \left(\bigcup_{r \in \mathcal{R}} \{x_{ref} \angle x \angle r\} \right), \quad (44)$$

where \mathcal{L} is a Lebesgue measure, notation $b \angle a$ means a dominates b (or b is dominated by a), and x_{ref} is a reference point dominated by all valid solutions in the solution set [9], [10].

For a given solution r_i , the S -metric identifies the size of space dominated by r_i but not dominated by any other solution, without loss of generality as:

$$S(r_i) = \Delta S(\mathcal{R}, r_i) = S(\mathcal{R}) - S(\mathcal{R} \setminus \{r_i\}). \quad (45)$$

In the optimization of classical communications, the existence of two objective functions is assumed. The first objective function, f_1 , is associated with the minimization of the cost

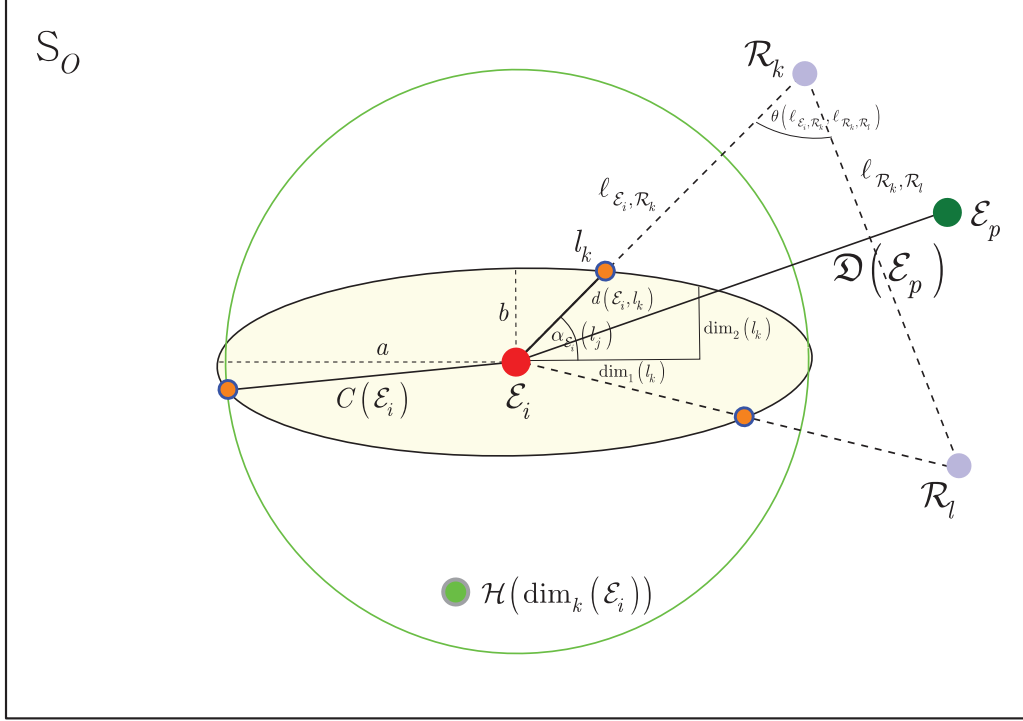


Fig. 2. Iteration step of the Poisson optimization model in the objective space S_O . An i^{th} epicenter, \mathcal{E}_i (depicted by the red dot), with a projected point l_k of random reference location \mathcal{R}_k . Reference locations \mathcal{R}_k and \mathcal{R}_l (blue dots) identify locations L_k and L_l , respectively. The power in \mathcal{R}_k is $P(\mathcal{E}_i, \mathcal{R}_k)$ (see (26)), while the magnitude is $M(\mathcal{E}_i, \mathcal{R}_k)$ (see (27)). Notation $\dim_i(\cdot)$ refers to the i^{th} dimension of l_k , and coefficients a and b define the shape of the ellipse (yellow) around epicenter \mathcal{E}_i . The $\mathcal{H}(\dim_k(\mathcal{E}_i))$ hypocentral of \mathcal{E}_i is determined via the range of the $C(\mathcal{E}_i)$ cumulative magnitude (depicted by the green circle). The new epicenter \mathcal{E}_p (depicted by the green dot) is determined by the $\mathcal{D}(\mathcal{E}_p)$ Poisson distance function using \mathcal{R}_k and \mathcal{R}_l , with angle $\theta(l_{\mathcal{E}_i, \mathcal{R}_k}, l_{\mathcal{R}_k, \mathcal{R}_l})$.

of the first type of classical communications related to the reception and storage of entangled systems in the quantum nodes (it covers the classical communications related to the required entanglement throughput by the nodes, fidelity of received entanglement, number of stored entangled states, and fidelity parameters). Thus,

$$f_1 : \min_{\forall i} \mathcal{C}_1(x_i), \quad (46)$$

where $\mathcal{C}_1(x_i)$ is the cost associated with the first type of classical communications related to a x_i .

The second objective function, f_2 , is associated with the cost of the second type of classical communications that is related to entanglement purification:

$$f_2 : \min_{\forall i} \mathcal{C}_2(x_i), \quad (47)$$

where $\mathcal{C}_2(x_i)$ is the cost associated with the second type of classical communications with respect to x_i .

Assuming objective functions f_1 and f_2 , the $S(r_i)$ of a particular solution r_i is as follows:

$$S(r_i) = (f_1(r_i) - f_1(r_{i-1})) (f_2(r_i) - f_2(r_{i+1})). \quad (48)$$

Given that the S -metric is calculated for the solutions, a set of nearest neighbors that restrict the space can be determined. Since the volume of this space can be quantified by the hypervolume, the solutions that satisfy objectives f_1 and f_2 can be found by utilizing (48).

F. Computational Complexity

The computational complexity of the Poissonian optimization method is derived as follows: Given that $|\mathcal{P}|$ epicenters are generated in the search space and that the number of locations for an i^{th} epicenter \mathcal{E}_i is determined by the dispersion operator $D(\mathcal{E}_i)$, the resulting computational complexity at a total number of locations $q = \sum_{i=1}^{|\mathcal{P}|} D(\mathcal{E}_i)$ (see (22)) is

$$\mathcal{O}\left((|\mathcal{P}| + q)^{d/2} \log(|\mathcal{P}| + q)\right), \quad (49)$$

since after a sorting process the locations for a given epicenter \mathcal{E}_i can be calculated with complexity $\mathcal{O}(D(\mathcal{E}_i))$, where d is the number of objectives.

Considering that in our setting $d = 2$, the total complexity is

$$\mathcal{O}\left((|\mathcal{P}| + q) \log(|\mathcal{P}| + q)\right). \quad (50)$$

IV. PROBLEM RESOLUTION

The resolution of the problem shown in Section II using the Poissonian entanglement optimization framework of Section III is as follows:

Let $X_{\mathcal{S}_{low}}$ be a set of nodes for which condition (7) holds for the fidelity of the received entangled states in the nodes, and let $X_{\mathcal{S}_{high}}$ be a set of nodes for which condition (8) holds for the received fidelity entanglement.

Then let $|X_{S_{low}}|$ and $|X_{S_{high}}|$ be the cardinality of $X_{S_{low}}$ and $X_{S_{high}}$, respectively.

Specifically, function (10) for the $X_{S_{low}}$ -type nodes is rewritten as

$$\mathcal{G}^{X_{S_{low}}}(\mathbf{X}) = \max \sum_{i=1}^{|X_{S_{low}}|} \mathcal{F}_i^{X_{S_{low}}}(\mathbf{X}) \mathbb{E} \left(D_i^{X_{S_{low}}}(\mathbf{X}) \right), \quad (51)$$

where $\mathcal{F}_i^{X_{S_{low}}}(X)$ is the entanglement fidelity function for an i^{th} $X_{S_{low}}$ -type node x_i , $x_i \in X_{S_{low}}$, and $\mathbb{E} \left(D_i^{X_{S_{low}}}(\mathbf{X}) \right)$ is the expected relative entropy of entanglement in an i^{th} $X_{S_{low}}$ -type x_i .

Similarly, for the $X_{S_{low}}$ -type nodes, function (10) is as follows:

$$\mathcal{G}^{X_{S_{high}}}(\mathbf{X}) = \max \sum_{i=1}^{|X_{S_{high}}|} \mathcal{F}_i^{X_{S_{high}}}(\mathbf{X}) \mathbb{E} \left(D_i^{X_{S_{high}}}(\mathbf{X}) \right). \quad (52)$$

From (51) and (52), a cumulative $\mathcal{G}^{X_{S_{high}} \otimes X_{S_{high}}}(\mathbf{X})$ is defined as

$$\begin{aligned} \mathcal{G}^{X_{S_{low}} \otimes X_{S_{high}}}(\mathbf{X}) &= \sum_{i=1}^{|X_{S_{high}}|} A_i \mathcal{F}_i^{X_{S_{high}}}(\mathbf{X}) \mathbb{E} \left(D_i^{X_{S_{high}}}(\mathbf{X}) \right) \\ &+ \sum_{i=|X_{S_{high}}|+1}^{|X_{S_{low}}|+|X_{S_{high}}|} A_i \mathcal{F}_i^{X_{S_{low}}}(\mathbf{X}) \mathbb{E} \left(D_i^{X_{S_{low}}}(\mathbf{X}) \right) F_1(\mathbf{X}), \end{aligned} \quad (53)$$

where A_i refers to the number of received entangled systems in an i^{th} node, while

$$F_1(\mathbf{X}) = \min \mathcal{C}(\mathbf{X}) = \sum_{i=1}^N \sum_{j=1}^T f_j B_F^j(x_i). \quad (54)$$

The fidelity types of the available resource states in the nodes should be further divided into T classes. The final function is then evaluated as

$$\begin{aligned} \mathcal{G}^{X_{S_{low}} \otimes X_{S_{high}}}(\mathbf{X}) &= F_1(\mathbf{X}) F_2(\mathbf{X}) \\ &= \sum_{i=1}^{|X_{S_{low}}|+|X_{S_{high}}|} \sum_{j=1}^T f_j B_F^j(x_i) F_2(\mathbf{X}), \end{aligned} \quad (55)$$

where

$$F_2(\mathbf{X}) = \min \mathcal{S}(\mathbf{X}) = \sum_{i=1}^{|X_{S_{low}}|+|X_{S_{high}}|} \mathcal{S}_i(\mathbf{X}). \quad (56)$$

Thus,

$$\mathcal{G}^{X_{S_{low}} \otimes X_{S_{high}}}(\mathbf{X}) = \sum_{i=1}^{|X_{S_{low}}|+|X_{S_{high}}|} \mathcal{S}_i(\mathbf{X}), \quad (57)$$

such that [9], [10]

$$\begin{aligned} \sum_{i=1}^{|X_{S_{low}}|+|X_{S_{high}}|} \mathcal{F}_i(\mathbf{X}) &\geq \gamma F_1(N) \\ &= \gamma \sum_{i=1}^{|X_{S_{low}}|+|X_{S_{high}}|} \sum_{j=1}^T f_j B_F^j(x_i) \\ &\leq \nu_{\mathbf{X}}(\varphi_i) \Lambda \leq \Pi B_F^j(x_i), \end{aligned} \quad (58)$$

where $\nu_{\mathbf{X}}(\varphi_i) = \sum_{j=1}^Z \tau_j(\varphi_i)$, γ is given by the constraint of (13), while Π is given by the constraint of (19).

A. Convergence of Solutions

Let $\mathcal{F}_i(\mathbf{X})$, $\mathcal{F}_i(\mathbf{X}) \in [0, 1]$ be the objective function that refers to the resulting entanglement fidelity in a particular node x_i , after purification and quantum error correction with per-node cost functions $F_1^i(\mathbf{X})$, $F_1^i(\mathbf{X}) \in [0, 1]$, and $F_2^i(\mathbf{X})$, $F_2^i(\mathbf{X}) \in [0, 1]$, respectively.

Precisely, a current i^{th} epicenter \mathcal{E}_i identifies a solution in the objective space $S_O : \{F_1^i(N), F_2^i(N), \mathcal{F}_i(\mathbf{X})\}$. The random locations around \mathcal{E}_i also represent possible solutions. Let \mathcal{E}^* be an optimal solution in the S_O subject space, which maximizes $\mathcal{F}_i(\mathbf{X})$ and minimizes $F_1^i(\mathbf{X})$ and $F_2^i(\mathbf{X})$. From \mathcal{E}_i , the algorithm determines a new solution (epicenter) \mathcal{E}_p via the $\mathcal{D}(\mathcal{E}_p)$ Poisson distance function, using the connection model between the locations around \mathcal{E}_i . To improve the diversity, locations around \mathcal{E}_p are generated. The new epicenter \mathcal{E}_p converges to an optimal solution \mathcal{E}^* . The iterations are repeated until \mathcal{E}^* is not found or until a stopping criterion is met.

The iteration from a current solution \mathcal{E}_i to a new solution \mathcal{E}_p toward a global optimal \mathcal{E}^* in S_O is illustrated in Fig. 3.

V. NUMERICAL EVIDENCE

In this section, a numerical evidence is proposed to demonstrate the Poisson entanglement optimization method.

A. Decision Making

To demonstrate the results of Section IV, let $\mathcal{F}_i(\mathbf{X})$ be the object function subject to maximize. The problem is to determine a matrix \mathbf{X} that maximizes $\mathcal{F}_i(\mathbf{X})$, and also $\mathbb{E} \left(D_i^{N_{S_{low}}}(\mathbf{X}) \right)$, and minimizes the cost functions $F_1^i(N)$ and $F_1^i(N)$. Thus, for each node N , the optimal number of received and stored entangled systems should be determined, with high and low fidelity classes.

Particularly, finding an optimal solution \mathcal{E}^* in S_O with the assumptions given Section IV, is therefore means the selection of the optimal objective function (e.g., maximizing the entanglement fidelity $\mathcal{F}_i(\mathbf{X})$ or maximizing the relative entropy of entanglement $\mathbb{E} \left(D_i^{N_{S_{low}}}(\mathbf{X}) \right)$), in particular node types $X_{S_{low}}$ and $X_{S_{high}}$, while all cost functions are minimized in the quantum network.

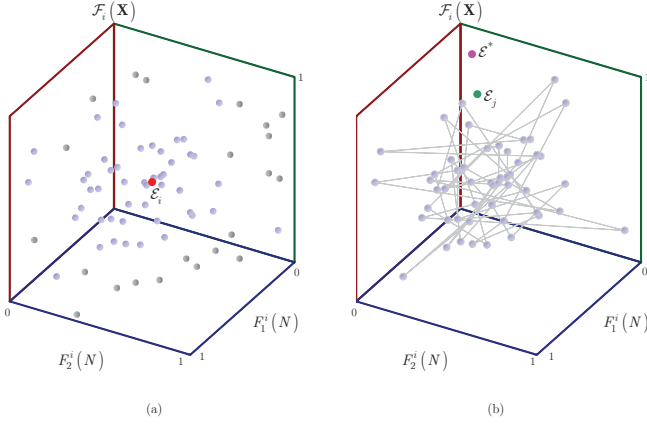


Fig. 3. Distribution of solutions for entanglement fidelity maximization in the objective space $S_O : \{F_1^i(N), F_2^i(N), \mathcal{F}_i(\mathbf{X})\}$ of the entanglement optimization problem (cost functions $F_1^i(N)$ and $F_2^i(N)$ and the objective function $\mathcal{F}_i(\mathbf{X})$ are normalized onto the range of $[0, 1]$). (a): A random epicenter \mathcal{E}_i refers to a current solution (depicted by the red dot) with the Poisson distributed reference locations (the reference points are not real solutions). The random reference locations are clustered into two classes: (1) reference locations within radius r (\mathcal{E}_i) around \mathcal{E}_i and (2) reference locations outside the radius (depicted by the gray dots). Reference locations outside the range are neglected in the iteration. (b): A new epicenter \mathcal{E}_p (depicted by the green dot) is determined via the connection model of relevant reference points (e.g., lie inside the range of r (\mathcal{E}_i)), which yields the $\mathcal{D}(\mathcal{E}_p)$ Poisson distance function. The new solution, \mathcal{E}_p , converges toward an optimal solution \mathcal{E}^* (depicted by the purple dot). The reference locations inside the relevance region are weighted by the seismic power function.

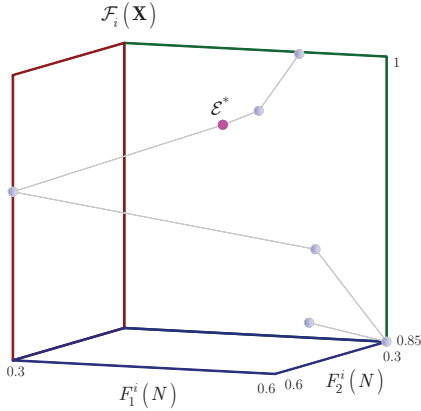


Fig. 4. Solution set in S_O , with an optimal epicenter \mathcal{E}^* , $F_1^i(N) \in [0.3, 0.6]$, $F_2^i(N) \in [0.3, 0.6]$, $\mathcal{F}_i(\mathbf{X}) \in [0.85, 1]$.

A solution set in S_O is depicted in Fig. 4.

An optimal solution \mathcal{E}^* in S_O therefore yields the maximization of entanglement fidelity $\mathcal{F}_N(X)$ if a particular node N belongs to the class $N_{S_{high}}$, whereas it maximizes the relative entropy of entanglement $\mathbb{E}\left(D_i^{N_{S_{low}}}(\mathbf{X})\right)$ if N belongs to the class $N_{S_{low}}$. Increasing $B_F^j(x_i)$ for a $N_{S_{high}}$ -class node and then performing an optimal purification and quantum error correction could significantly improve the fidelity of entanglement. On the other hand, for a $N_{S_{low}}$ -class node, the fidelity improvement at an optimal purification and quantum error correction is insignificant. Thus, incrementing $B_F^j(x_i)$ cannot improve the fidelity. The optimal solution for these nodes is

to focus on improving the relative entropy of entanglement, which requires lower cost function values.

This decision strategy provides a global optimal with respect to all quantum nodes of the quantum network.

B. Distribution of Solutions

First, we analyze the distribution of solutions in the feasible space S_F focusing on the magnitudes associated to the locations around epicenters.

Let assume that the total number of q locations (see (22)) can be divided into m magnitude ranges [11], such that

$$\sum_{i=1}^m n_i = q = \sum_{i=1}^{|\mathcal{P}|} D(\mathcal{E}_i), \quad (59)$$

where n_i is the number of locations belonging to an i^{th} magnitude range, $|\mathcal{P}|$ is the population size. Then let M_i be the magnitude associated to the i^{th} magnitude range. Then a \tilde{n}_i approximation of n_i is evaluated as

$$\tilde{n}_i = f(M_i), \quad (60)$$

where $f(\cdot)$ is a fitting function. To give an estimate on n_i at a particular magnitude M_i , we utilize a power law distribution [11] function $\mathcal{B}(n_i)$ for a log-scaled n_i , as

$$\mathcal{B}(n_i) : \log_{10}(n_i) = a - b\tilde{M}_i, \quad (61)$$

where \tilde{M}_i is a log scaled M_i , while a and b are constants [11].

Then, the \tilde{n}_i Poisson estimate is yielded as

$$\tilde{n}_i = \sigma_i^2 = \lambda_i, \quad (62)$$

where σ_i^2 is the observational variance, while λ_i is the mean of a Poisson distribution. Since the sum of independent Poisson variables is also a Poisson variable with mean equals to the sum of the components means,

$$\lambda(q) = \sum_{i=1}^m \lambda_i \approx q, \quad (63)$$

where $\lambda(q)$ is the mean total number, while λ_i is an i^{th} component mean. Using the Poisson property $\sigma^2 = \lambda$, the σ_q^2 estimated uncertainty is yielded as [11] $\sigma_q^2 = \lambda(q) = \sum_{i=1}^m f(\tilde{M}_i)$. Thus using a corresponding fitting function $f(\cdot)$, the mean and the variance of the total number of events are equal to the sum of the fitted values.

In our model the distribution of the log scaled $\tilde{n}_i = \lambda_i$ values in function of M_i are well approachable by the power law distribution $\mathcal{B}(\lambda_i) : \log_{10}(\lambda_i) = a - b\tilde{M}_i$, while the distribution of the $\lambda(q)$ total number (63) of locations are approachable by a $\mathcal{N}(\lambda(q), \sigma_N^2)$, Gaussian distribution with variance $\sigma_N^2 = \lambda(q)$ as $\lambda(q) \rightarrow \infty$, by theory.

A distributions of $\mathcal{B}(\lambda_i)$ in function of the magnitude M_i and coefficient b are illustrated in Fig. 5.

The distributions of $\lambda(q)$ (see (63)) for k_{it} iterations are depicted in Fig. 6. In Fig. 6(a), $\lambda(q) = 10^2$, while Fig. 6(b) illustrated the distribution at $\lambda(q) = 10^6$. As $\lambda(q) \rightarrow \infty$, the distributions of $\lambda(q)$ can be approximated by a $\mathcal{N}(\lambda(q), \sigma_N^2)$, $\sigma_N^2 = \lambda(q)$ Gaussian distribution.

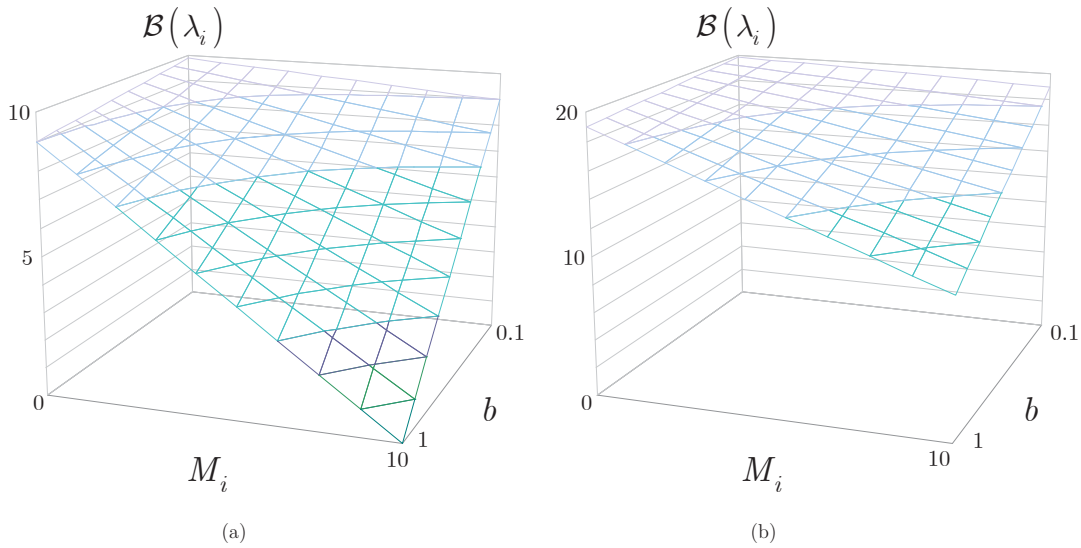


Fig. 5. Distribution of $\mathcal{B}(\lambda_i)$ for different magnitudes M_i , $M_i = 1, \dots, 10$ and coefficient b , for (a): $a = 10$, and (b): $a = 20$.

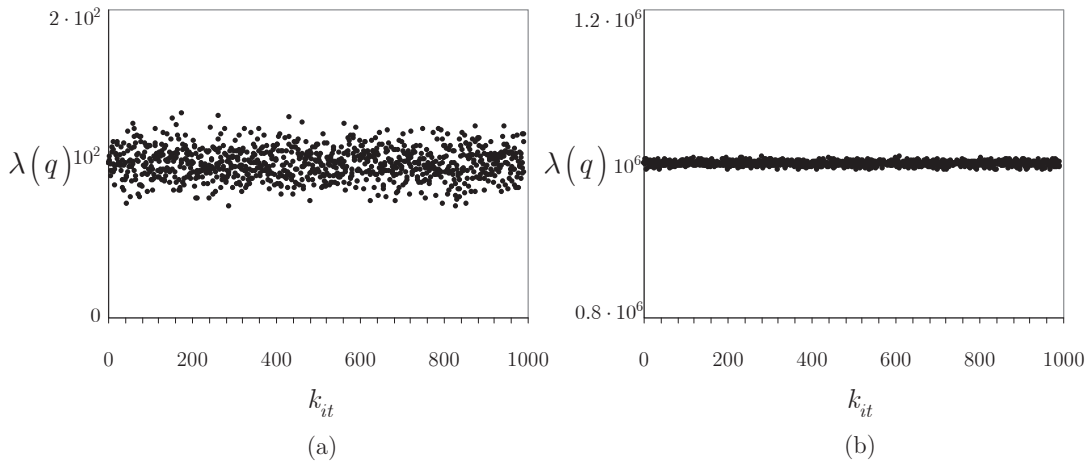


Fig. 6. Distribution of $\lambda(q)$ for k_{it} iterations, $k_{it} = 0, \dots, 1000$, for (a): $\lambda(q) = 10^2$, and (b): $\lambda(q) = 10^6$.

The associated distributions of $\mathcal{B}(\lambda_i)$ for the values of $\lambda(q)$ are depicted in Fig. 7. The maximum value of $\mathcal{B}(\lambda_i)$ is selected to $\mathcal{B}(\lambda_i) \approx 10$ in each cases which values are picked up at $\lambda(q)$, where $\lambda(q) = 10^2$ in Fig. 7(a), and $\lambda(q) = 10^6$ in Fig. 7(b). The $\mathcal{B}(\lambda_i)$ values approximates to a Gaussian distribution. The statistical distribution of $\mathcal{B}(\lambda_i)$ is therefore constitutes a similar pattern for arbitrary $\lambda(q)$.

VI. CONCLUSIONS

The proposed Poissonian entanglement optimization framework fuses the fundamental concepts of quantum Shannon theory with the theory of evolutionary algorithms and seismic wave propagations. Two objective functions are defined, with primary focus on the entanglement fidelity and secondary focus on the relative entropy of entanglement. As an additional objective function, the minimization of classical communications required by the entanglement optimization procedure is considered. The cost functions are defined to cover the

physical attributes of entanglement transmission, purification, and storage in quantum memories. This method can be implemented with low complexity that allows a straightforward application in future quantum Internet and quantum networking scenarios.

REFERENCES

- [1] R. Van Meter, *Quantum Networking*, John Wiley and Sons Ltd, ISBN 1118648927, 9781118648926 (2014).
- [2] L. Gyongyosi, S. Imre and H. V. Nguyen, A Survey on Quantum Channel Capacities, *IEEE Communications Surveys and Tutorials* **99**, 1, doi: 10.1109/COMST.2017.2786748 (2018).
- [3] S. Lloyd, J.H. Shapiro, F.N.C. Wong, P. Kumar, S.M. Shahriar, and H.P. Yuen. Infrastructure for the quantum Internet, *ACM SIGCOMM Computer Communication Review*, 34(5):9–20, (2004).
- [4] H. J. Kimble, The quantum internet, *Nature* **453**, 1023 - 1030 (2008).
- [5] R. Van Meter, T. Satoh, T. D. Ladd, W. J. Munro, K. Nemoto, Path Selection for Quantum Repeater Networks, *Networking Science*, Vol. 3, Issue 1-4, pp 82-95 (2013).
- [6] R. Van Meter, T. D. Ladd, W.J. Munro, K. Nemoto, System Design for a Long-Line Quantum Repeater, *IEEE/ACM Transactions on Networking* **17**(3), 1002-1013, (2009).

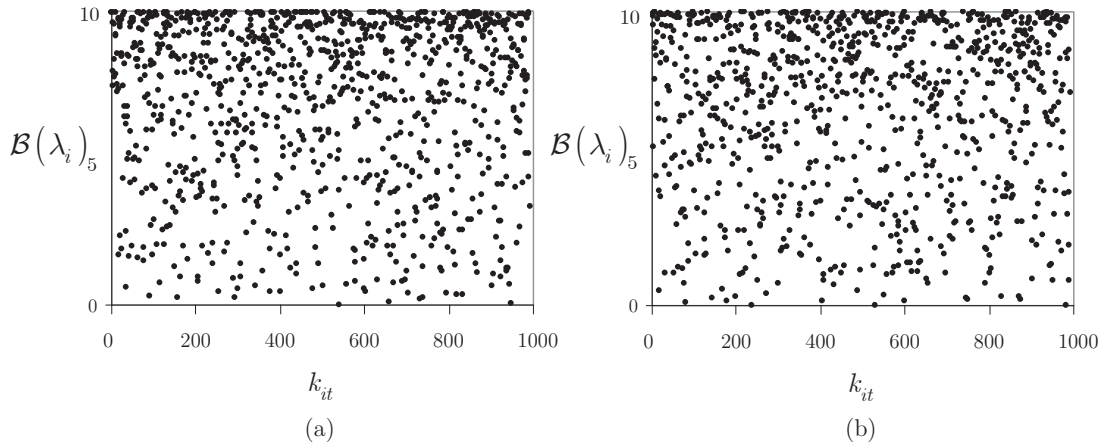


Fig. 7. The distributions of $\mathcal{B}(\lambda_i)$ for k_{it} iterations, $k_{it} = 0, \dots, 1000$, (a): $\lambda(q) = 10^2$, and (b): $\lambda(q) = 10^6$.

- [7] S. Imre and L. Gyongyosi. *Advanced Quantum Communications - An Engineering Approach*. Wiley-IEEE Press (New Jersey, USA), (2013).
- [8] S. Pirandola, Capacities of repeater-assisted quantum communications, *arXiv:1601.00966* (2016).
- [9] Y. Tan, *Fireworks Algorithm, A Novel Swarm Intelligence Optimization Method*, Springer (2015).
- [10] Y.J. Zheng, Q. Song, S.Y. Chen, Multiobjective fireworks optimization for variable-rate fertilization in oil crop production. *Appl. Soft Comput.* 13(11), 4253–4263 (2013).
- [11] J. Greenhough, I. G. Main, A Poisson model for earthquake frequency uncertainties in seismic hazard analysis, *arXiv:0807.2396v2 DOI 10.1029/2008GL035353* (2008).
- [12] S. Kannan, Improving Innovative Mathematical Model for Earthquake Prediction, *J Geol Geosci* 2014, <http://dx.doi.org/10.4172/2329-6755.1000168> (2014).
- [13] J. Mejia, K. Rojas, N. Valeza, A. R. Villagrancia, Earthquake prediction through Kannan-Mathematical-Model Analysis and Dobrovolsky-based clustering Technique, *DLSU Research Congress 2015* (2015).
- [14] S. G. Stamatovska, The Latest Mathematical Models of Earthquake Ground Motion, *Seismic Waves - Research and Analysis*, InTech (2012).
- [15] Xiao, Y.F., Gong, Q. Optical microcavity: from fundamental physics to functional photonics devices, *Science Bulletin*. 61(3): 185-186 (2016).
- [16] Zhang et al. Quantum Secure Direct Communication with Quantum Memory. *Phys. Rev. Lett.* 118, 220501 (2017).
- [17] Biamonte, J. et al. Quantum Machine Learning. *Nature*, 549, 195-202 (2017).
- [18] Lloyd, S. Mohseni, M. & Rebentrost, P. Quantum algorithms for supervised and unsupervised machine learning. *arXiv:1307.0411* (2013).
- [19] Chou, C., Laurat, J., Deng, H., Choi, K.S., de Riedmatten, H., Felinto, D. & Kimble, H.J. Functional quantum nodes for entanglement distribution over scalable quantum networks. *Science*, 316(5829):1316–1320 (2007).
- [20] Sheng, Y. B., Zhou, L. Distributed secure quantum machine learning. *Science Bulletin* (2017).
- [21] Kok, P., Munro, W.J., Nemoto, K., Ralph, T.C., Dowling, J.P. & Milburn, G.J. Linear optical quantum computing with photonic qubits. *Rev. Mod. Phys.* 79, 135-174 (2007).

APPENDIX

A. Definitions

1) *Entanglement Fidelity*: The fidelity for two pure quantum states is defined as

$$F(|\varphi\rangle, |\psi\rangle) = |\langle\varphi|\psi\rangle|^2. \quad (\text{A.1})$$

The fidelity of quantum states can describe the relation of a pure channel input state $|\psi\rangle$ and the received mixed quantum

system $\sigma = \sum_{i=0}^{n-1} p_i \rho_i = \sum_{i=0}^{n-1} p_i |\psi_i\rangle\langle\psi_i|$ at the channel output as

$$F(|\psi\rangle, \sigma) = \langle\psi|\sigma|\psi\rangle = \sum_{i=0}^{n-1} p_i |\langle\psi|\psi_i\rangle|^2. \quad (\text{A.2})$$

Fidelity can also be defined for mixed states ρ and σ

$$F(\rho, \sigma) = (\text{Tr}(\sqrt{\sqrt{\sigma}\rho\sqrt{\sigma}}))^2 = \sum_i p_i (\text{Tr}(\sqrt{\sqrt{\sigma_i}\rho_i\sqrt{\sigma_i}}))^2. \quad (\text{A.3})$$

2) *Relative Entropy of Entanglement*: By definition, the $E(\rho)$ relative entropy of entanglement function of a joint state ρ of subsystems A and B is defined by the $D(\cdot|\cdot)$ quantum relative entropy function, without loss of generality as

$$E(\rho) = \min_{\rho_{AB}} D(\rho|\rho_{AB}) = \min_{\rho_{AB}} \text{Tr}(\rho \log \rho) - \text{Tr}(\rho \log(\rho_{AB})), \quad (\text{A.4})$$

where ρ_{AB} is the set of separable states $\rho_{AB} = \sum_{i=1}^n p_i \rho_{A,i} \otimes \rho_{B,i}$.

B. Evaluation of Solutions

1) *Fitness Function*: To evaluate the performance of the epicenters we utilize a mathematical apparatus based on the Pareto strength and fitness assignment [9], [10].

Let $\text{Pr}(\mathcal{E}_i)$ be the probability of selection of an epicenter \mathcal{E}_i , defined as

$$\text{Pr}(\mathcal{E}_i) = \frac{\kappa(\mathcal{E}_i)}{\sum_{l \in K} \kappa(\mathcal{E}_l)}, \quad (\text{A.5})$$

where $\kappa(\mathcal{E}_i)$ is the sum of $d(\cdot)$ Euclidean distances between \mathcal{E}_i and the other epicenters, as

$$\kappa(\mathcal{E}_i) = \sum_{l=1}^K d(\mathcal{E}_i, \mathcal{E}_l) = \sum_{l=1}^K \|\mathcal{E}_i - \mathcal{E}_l\|, \quad (\text{A.6})$$

where K is a set with cardinality

$$|K| = \sum_{i=1}^{|\mathcal{P}|} D(\mathcal{E}_i) + \sum_{i=1}^N \sum_{k=1}^{\dim(\mathcal{E}_i)} R(i, k), \quad (\text{A.7})$$

where $D(\mathcal{E}_i)$ is given in (21), and $l \in K$ refers to that the position of \mathcal{E}_j belongs to set K , and $|\mathcal{P}|$ is the population size. Let \mathcal{NP} refer to the non-dominated solution archive, and let

$$\varphi_i = \mathcal{E}_i \quad (\text{A.8})$$

refer to the selected epicenter, i.e., to an individual solution in \mathcal{P} or in \mathcal{NP} .

Let $\Phi(\varphi_i)$ be a strength coefficient for solution φ_i , defined as

$$\Phi(\varphi_i) = \left| \varphi_k \in \mathcal{P} \cup \mathcal{NP} \mid \varphi_k \angle \varphi_i \right|, \quad (\text{A.9})$$

where \angle refers to the Pareto dominance relation between φ_i and $\varphi_k = \mathcal{E}_k$. As follows, (A.9) depends on the number of individuals it dominates, by theory [9], [10].

By definition, a decision vector \mathbf{A} dominates a vector \mathbf{B} , i.e., $\mathbf{B} \angle \mathbf{A}$, if

$$f_i(\mathbf{A}) \leq f_i(\mathbf{B}) \quad (\text{A.10})$$

for $\forall i, i = 1, \dots, m$ and for at least one j with $i, j = 1, \dots, n$,

$$f_j(\mathbf{A}) \leq f_j(\mathbf{B}), \quad (\text{A.11})$$

where $f: \mathbb{R}^m \rightarrow \mathbb{R}^n$. The set of non-dominated decision vectors in \mathbb{R}^n is called a Pareto optimal set, while the image under f in the solution space is called the Pareto front [9], [10]. In a multiobjective optimization the aim is to achieve the best Pareto front, by theory.

Using (A.9), let $\alpha(\varphi_i)$ be the raw fitness value of φ_i evaluated by the $\Phi(\cdot)$ strength function (see (A.9)) of its dominators as

$$\alpha(\varphi_i) = \sum_{(\varphi_k \in \mathcal{P} \cup \mathcal{NP}) \wedge (\varphi_i \angle \varphi_k)} \Phi(\varphi_k), \quad (\text{A.12})$$

with an inverse distance function (referred to as the density value of φ_i), $\rho(\varphi_i)$ as

$$\rho(\varphi_i) = \frac{1}{d_g(\varphi_i)}, \quad (\text{A.13})$$

where $d_g(\varphi_i)$ is the distance from solution φ_i to its g^{th} nearest individual, where g is initialized as the square root of the sample size $|\mathcal{P} \cup \mathcal{NP}|$, by theory [9], [10].

Using (A.13), a for a random solution $r(\varphi_i)$ the $\tilde{f}(\cdot)$ fitness function of φ_i is as

$$\tilde{f}(\varphi_i) = \alpha(\varphi_i) + \rho(\varphi_i). \quad (\text{A.14})$$

Then let p refer to the number of selected φ_i solutions in \mathcal{P} . Using (A.14), the selection probability of each solution is yielded as

$$\Pr(\varphi_i) = \frac{\tilde{f}(\varphi_i)}{\sum_{r \in \mathcal{P}} \tilde{f}(\varphi_r)}. \quad (\text{A.15})$$

2) *Constraints*: As a solution φ_i does not satisfy the problem constraints C_1, C_2, C_3 , a $H^{C_z}(\varphi_i)$, $z = 1, 2, 3$ degrees of violation are defined for the constraints.

For constraint C_1 (see (13)), the $H^{C_1}(\varphi_i)$ violation function [9], [10] is as

$$H^{C_1}(\varphi_i) = \begin{cases} \gamma - \zeta(\varphi_i), & \text{if } \zeta(\varphi_i) \leq \gamma \\ 0, & \text{otherwise,} \end{cases} \quad (\text{A.16})$$

where

$$\zeta(\varphi_i) = \sum_{i=1}^N \mathcal{F}_i(\varphi_i). \quad (\text{A.17})$$

For constraint C_2 (see (15)), the $H^{C_2}(\varphi_i)$ violation function is as follows

$$H^{C_2}(\varphi_i) = \begin{cases} F_1(\varphi_i) - \Lambda, & \text{if } F_1(\varphi_i) \geq \Lambda \\ 0, & \text{otherwise,} \end{cases} \quad (\text{A.18})$$

where

$$F_1(\varphi_i) = \sum_{i=1}^N \sum_{i=1}^T f_j B_F^j(\varphi_i). \quad (\text{A.19})$$

For constraint C_3 (see (19)), the $H^{C_3}(\varphi_i)$ violation function is as

$$H^{C_3}(\varphi_i) = \begin{cases} \nu(\varphi_i) - \Pi, & \text{if } \nu(\varphi_i) \geq \Pi \\ 0, & \text{otherwise,} \end{cases} \quad (\text{A.20})$$

where

$$\nu(\varphi_i) = \sum_{j=1}^N \tau_j(\varphi_i). \quad (\text{A.21})$$

From (A.16), (A.18) and (A.20) a penalty coefficient $\partial(\varphi_i)$ is defined as

$$\partial(\varphi_i) = w_1 H^{C_1}(\varphi_i) + w_2 H^{C_2}(\varphi_i) + w_3 H^{C_3}(\varphi_i), \quad (\text{A.22})$$

where w_i -s are weighting coefficients [9], [10].

3) *Selection Condition*: Assuming that there are χ number of selected random solutions such that the selection probabilities are proportional to their fitness values. The selection of a solution φ_i is as follows.

First from the selected random solutions a mutant solution \tilde{h}_i is generated as

$$\tilde{h}_i = \varphi_{r_a} + \vartheta(\varphi_{r_b} - \varphi_{r_c}), \quad (\text{A.23})$$

where $r_i \in \{a, \dots, p\}$ are the random indexes, while $\vartheta > 0$ is a coefficient.

From the components of \tilde{h}_i a trial solution T_i is defined with a j^{th} component $T_i^{(j)}$ as

$$T_i^{(j)} = \begin{cases} \tilde{h}_i^{(j)} & \text{if } r(0, 1) < P_{\text{cross}}, \text{ or } j = r(i) \\ \varphi_i^{(j)}, & \text{otherwise,} \end{cases} \quad (\text{A.24})$$

where $r(0, 1)$ is a random number from the range $[0, 1]$, $r(i)$ is a random integer within $(0, X]$ for each i , while P_{cross} is the crossover probability ranged in $(0, 1)$.

Then the selection of the solution φ_i using the trial solution T_i is as

$$\varphi_i = \begin{cases} T_i, & \text{if } \tilde{f}(T_i) \leq \tilde{f}(\varphi_i) \\ \varphi_i, & \text{otherwise,} \end{cases} \quad (\text{A.25})$$

where function $\tilde{f}(\cdot)$ is given in (A.14).

C. Sub-Procedure 1

The Sub-procedure 1 of Algorithm 1 is as follows [9], [10].

Sub-procedure 1 *Convergence of Solutions*

Apply feasible space exploration (41) through the dimensions $L_r^{\dim_k(\mathcal{E}_i)}$ around $\dim_k(\mathcal{E}_i)$ of the epicenters. For $i = 1, \dots, p$ obtain a T_i trial solution (A.24) for φ_i . Determine the best solution between φ_i and T_i via (A.25). If $\tilde{f}(T_i) \leq \tilde{f}(\varphi_i)$ and T_i is a non-dominated solution, then update \mathcal{NP} with T_i . Then, update \mathcal{P} with the best solution, and with other $p - 1$ randomly selected solutions, φ_q , $q = 1, \dots, p - 1$, using the selection probability function (A.5) as $\Pr(\varphi_q) = \tilde{f}(\varphi_q) / \sum_{i=1}^{p-1} \tilde{f}(\varphi_i)$.

D. Notations

The notations of the manuscript are summarized in Table A.1.

TABLE A.1: Summary of notations.

<i>Notation</i>	<i>Description</i>
l	Level of entanglement.
F	Fidelity of entanglement.
N	Number of nodes in the network.
T	Number of fidelity types F_j , $j = 1, \dots, T$ of the entangled states.
S_O	Objective space.
S_F	Feasible space.
L_l	An l -level entangled link. For an L_l link, the hop-distance is 2^{l-1} .
$d(x, y)_{L_l}$	Hop-distance of an l -level entangled link between nodes x and y .
$E_{L_l}(x, y)$	Entangled link $E_{L_l}(x, y)$ between nodes x and y .
$B_F(E_{L_l}(x, y))$	Entanglement throughput of an L_l -level entangled link $E_{L_l}(x, y)$ between nodes (x, y) .
$B_F^j(x_i)$	Number of incoming entangled states in an i^{th} node x_i , with fidelity-type j , $i = 1, \dots, N$.
\mathbf{X}	An $N \times T$ matrix, $\mathbf{X} = \left(B_F^j(x_i) \right)_{N \times T}$, it describes the number of resource entangled states injected into the nodes from each fidelity-type in the network, $B_F^j(x_i) \geq 0$ for all i and j .
$\mathcal{F}(x_i)$	A primary objective function. It identifies the cumulative entanglement fidelity (a sum of entanglement fidelities in x_i) after an entanglement purification $P(x_i)$ and an optimal quantum error correction $C(x_i)$ in x_i .
$P(x_i)$	Entanglement purification in x_i .
$C(x_i)$	Optimal quantum error correction in x_i .
$\langle B \rangle_F^j(x_i)$	An initialization value for $B_F^j(x_i)$ in a particular node x_i .
$\mathbb{E}(D_i(\mathbf{X}))$	A secondary objective function. It refers to the expected amount of cumulative relative entropy of entanglement (a sum of relative entropy of entanglement) in node x_i ,
$w_j(x_i)$	Quantum memory coefficient for the storage of entangled states from the j^{th} fidelity type in a node x_i , evaluated as: $w_j(x_i) = \eta_j B_F^j(x_i) + \kappa_j \langle B \rangle_F^j(x_i)$, where η_j and κ_j are coefficients to describe the storage characteristic of entangled states with the j^{th} fidelity type.
$\tau_j(\mathbf{X})$	Differentiation of storage characteristic of entangled states from the j^{th} fidelity type, defined as $\tau_j(\mathbf{X}) = \sum_{i=1}^N (w_j(x_i) - \Omega)^2$, where $\Omega = \sum_{i=1}^N w_j(x_i) / N$.
$f_C(P(x_i))$	Cost of entanglement purification $P(x_i)$ in x_i .
$f_C(C(x_i))$	Cost of optimal quantum error correction $C(x_i)$ in x_i .

$\mathcal{C}(\mathbf{X})$	Total cost function, defined as $\mathcal{C}(\mathbf{X}) = \sum_{i=1}^N f_C(P(x_i)) + f_C(C(x_i))$ $= \sum_{i=1}^N \sum_{j=1}^T f_j B_F^j(x_i),$ where T is the number of fidelity types, N is the number of nodes, f_j is a total cost of purification and error correction associated to the j^{th} fidelity type of entangled states.
f_j	Total cost of purification and error correction associated to the j^{th} fidelity type of entanglement fidelity.
F^*	Critical fidelity coefficient.
$\mathcal{S}_{low}, \mathcal{S}_{high}$	Sets with fidelity bounds $\mathcal{S}_{low}(F)$ and $\mathcal{S}_{high}(F)$ as $\mathcal{S}_{low}(F) : \max_{\forall i} F_i < F^*$, and $\mathcal{S}_{high}(F) : \min_{\forall i} F_i \geq F^*$.
$X_{\mathcal{S}_{low}}$	Set of nodes for which condition $\mathcal{S}_{low}(F) : \max_{\forall i} F_i < F^*$ holds.
$X_{\mathcal{S}_{high}}$	Set of nodes for which condition $\mathcal{S}_{high}(F) : \min_{\forall i} F_i \geq F^*$ holds.
$\mathcal{S}_i(\mathbf{X})$	Cost of quantum memory usage in node x_i , defined as $\mathcal{S}_i(\mathbf{X}) = \lambda \sum_{j=1}^T \alpha_i \frac{1}{\Upsilon_i} B_F^j(x_i),$ where λ is a constant, α_i is a quality coefficient, while Υ_i is a capacity coefficient of the quantum memory.
$\mathcal{G}(\mathbf{X})$	Main objective function, $\mathcal{G}(\mathbf{X}) = \max \sum_{i=1}^N \mathcal{F}_i(\mathbf{X}) \mathbb{E}(D_i(\mathbf{X})).$
$F_1(N)$	Minimization function for cost $\mathcal{C}(\mathbf{X})$.
$F_2(N)$	Minimization function for cost $\mathcal{S}(\mathbf{X})$.
C_1, C_2, C_3	Problem constraints.
\mathcal{E}	Epicenter, represents a solution in the feasible space.
L_j	A a random location around epicenter \mathcal{E} .
$D(\mathcal{E})$	Dispersion coefficient of an epicenter \mathcal{E} (solution in the feasible space). It determines the number of affected L_j , $j = 1, \dots, D(\mathcal{E})$, locations (also represent solutions in the feasible space) around an epicenter \mathcal{E} .
\mathcal{P}	Population \mathcal{P} (a set of possible solutions).
m	Control parameter.
\mathcal{E}_i	An i^{th} individual (epicenter) from the $ \mathcal{P} $ individuals (epicenters) in the population \mathcal{P} .
$\tilde{f}(\cdot)$	Fitness function.
$\tilde{f}(\langle \mathcal{E} \rangle)$	A maximum objective value among the $ \mathcal{P} $ individuals.
ϑ	A residual quantity.
$f_R(\cdot)$	Rounding function.
q	Total number of locations, $q = \sum_{i=1}^{ \mathcal{P} } D(\mathcal{E}_i)$.
$\hat{D}(\mathcal{E}_i)$	Upper bound on $D(\mathcal{E}_i)$ for a given epicenter \mathcal{E}_i .

$d(\mathcal{E}_i, l_j)$	Euclidean distance $d(\mathcal{E}_i, l_j)$ between an i^{th} epicenter \mathcal{E}_i and the projection point l_j of a j^{th} location point $L_j, j = 1, \dots, D(\mathcal{E})$ on the ellipsoid around \mathcal{E}_i .
$\dim_i(\cdot)$	An i^{th} dimension of l_j .
$P(\mathcal{E}_i, L_j)$	Seismic power $P(\mathcal{E}_i, L_j)$ operator for an i^{th} epicenter \mathcal{E}_i . Measures the power in a j^{th} location point $L_j, j = 1, \dots, D(\mathcal{E}_i)$, as $P(\mathcal{E}_i, L_j) = \left(\frac{1}{d(\mathcal{E}_i, l_j)} M(\mathcal{E}_i, L_j) \right)^{b_1} b_0 e^{\sigma_{\ln P(\mathcal{E}_i, L_j)}},$ where b_0 and b_1 are regression coefficients, $\sigma_{\ln P(\mathcal{E}_i, L_j)}$ is the standard deviation, while $M(\mathcal{E}_i, L_j)$ is the seismic magnitude in a location L_j , while l_j is the projection of L_j onto the ellipsoid around \mathcal{E}_i .
$M(\mathcal{E}_i, L_j)$	Magnitude between epicenter \mathcal{E}_i and location L_j is evaluated as $M(\mathcal{E}_i, L_j) = \left(P(\mathcal{E}_i, L_j) \frac{1}{b_0 e^{\sigma_{\ln P(\mathcal{E}_i, L_j)}}} \right)^{\frac{1}{b_1}} d(\mathcal{E}_i, l_j).$
$P^*(\mathcal{E}_i)$	Maximal seismic power for a given epicenter \mathcal{E}_i .
$C(\mathcal{E}_i)$	Cumulative magnitude for an epicenter \mathcal{E}_i .
\mathcal{E}'	Highest seismic power epicenter with magnitude $M(\mathcal{E}', L_j^{\mathcal{E}'})$.
$\tilde{f}(\mathcal{E}')$	Minimum objective values among the $ \mathcal{P} $ epicenters.
\mathcal{M}	Control parameter, $\mathcal{M} = \sum_{i=1}^{ \mathcal{P} } M(\mathcal{E}_i, L_j^{\mathcal{E}_i}),$ where $L_j^{\mathcal{E}_i}$ provides the maximal seismic power for an i^{th} epicenter \mathcal{E}_i
$\Phi(\mathcal{E}_i, \mathcal{R}_k, \mathcal{R}_l)$	Poisson range identifier function of \mathcal{E}_i , where \mathcal{R}_k and \mathcal{R}_l are random reference points.
$c_w(\mathcal{E}_i, \mathcal{R}_k), c_w(\mathcal{R}_k, \mathcal{R}_l)$	Weighting coefficients between epicenters \mathcal{E}_i and \mathcal{R}_k , and between \mathcal{R}_k and \mathcal{R}_l .
$\mathfrak{D}(\mathcal{E}_p)$	Poissonian distance function $\mathfrak{D}(\mathcal{E}_p)$, where \mathcal{E}_p is a new solution.
$r(\mathcal{E}_i)$	Radius around a current solution \mathcal{E}_i , defined as $r(\mathcal{E}_i) = \chi 10^{Q_1(2\tilde{M}) - Q_2},$ where \tilde{M} is the average magnitude $\tilde{M} = \frac{1}{ \mathcal{P} } \mathcal{M} = \frac{1}{ \mathcal{P} } \sum_{i=1}^{ \mathcal{P} } M(\mathcal{E}_i, L_j^{\mathcal{E}_i}),$ while Q_1 and Q_2 are constants, while χ is a normalization term.
$\dim_k(\mathcal{E}_i)$	Randomly selected k^{th} dimension, $k = 1, \dots, \dim(\mathcal{E}_i)$ of a current epicenter $\mathcal{E}_i, i = 1, \dots, \mathcal{P} $.
$\mathcal{H}(\dim_k(\mathcal{E}_i))$	Hypocentral, provides a random displacement of $\dim_k(\mathcal{E}_i)$ using $C(\mathcal{E}_i)$.
$L_r^{\dim_k(\mathcal{E}_i)}$	A random location in the k^{th} dimension $L_r^{\dim_k(\mathcal{E}_i)}$ around $\dim_k(\mathcal{E}_i)$.
$N(\cdot)$	Normalization operator $N(\cdot)$ of $L_r^{\dim_k(\mathcal{E}_i)}$. It keeps the new locations around $\dim_k(\mathcal{E}_i)$ in \mathcal{S}_F , where B_{low}^k and B_{up}^k are lower and upper bounds on the boundaries of locations in a k^{th} dimension.
S -metric	Hypervolume indicator. A quality measure for the solutions or a contribution of a single solution in a solution set.

$S(\mathcal{R})$	S -metric for a solution set $\mathcal{R} = \{r_1, \dots, r_n\}$ is as $S(\mathcal{R}) = \mathcal{L}(\bigcup_{r \in \mathcal{R}} \{x_{ref} \angle x \angle x r\})$, where \mathcal{L} is a Lebesgue measure, notation $b \angle a$ refers to that a dominates b (or b is dominated by a), while x_{ref} is a reference point dominated by all valid solutions in the solution set.
f_1, f_2	Objective function.
$\mathcal{C}_1(x_i)$	Cost results from the first-type classical communications related to a x_i .
$\mathcal{C}_2(x_i)$	Cost results from the second-type classical communications with respect to x_i .
\mathcal{E}^*	Global optima.
m	Number of magnitude ranges.
n_i	Number of locations belonging to an i^{th} magnitude range.
$\mathcal{B}(n_i)$	Power law distribution function for a log-scaled n_i , $\mathcal{B}(n_i) : \log_{10}(n_i) = a - b\tilde{M}_i$, where \tilde{M}_i is a log scaled M_i , while a and b are constants.
\tilde{n}_i	Poisson estimate of n_i , as $\tilde{n}_i = \sigma_i^2 = \lambda_i$, where σ_i^2 is the observational variance, while λ_i is the mean of a Poisson distribution.
σ_q^2	Estimated uncertainty, $\sigma_q^2 = \lambda(q) = \sum_{i=1}^m f(\tilde{M}_i)$, where $f(\cdot)$ is a fitting function.
$\lambda(q)$	Mean total number, $\lambda(q) = \sum_{i=1}^m \lambda_i \approx q$, where λ_i is an i^{th} component mean.
$\mathcal{B}(\lambda_i)$	Power law distribution function for $\lambda_i = \tilde{n}_i$.
k_{it}	Number of iterations.